Response of a steady-state critical wedge orogen to changes in climate and tectonic forcing

Gerard H. Roe, Drew R. Stolar, and Sean D. Willett

January 31, 2004

Abstract

The theories of critical orogenic wedges and fluvial erosion are combined to explore the interactions between tectonics, erosion, and climate. A model framework is developed which allows the derivation of an exact analytical scaling relationship for how orogen width, height, and rock uplift rate varies as a function of accretionary flux and precipitation rate. Compared to a model with prescribed uplift rate, incorporating the tectonic response introduces a powerful negative feedback on the orogen, which strongly damps the systems equilibrium response to changes in forcing. Furthermore, for the most commonly assumed forms of the fluvial erosion law, the orogen is more sensitive to changes in the accretionary flux than in the precipitation rate. And while increases in accretionary flux and precipitation rate both cause an increase in exhumation rate, they have opposite tendencies on the orogen relief. Further analysis shows that the pattern of rock uplift does not affect the scaling relationship and that it is only weakly dependent on the hillslope condition.

1 Introduction

That the mountainous terrains on Earth are shaped by the triumvirate of climate, erosion, and tectonics is one of the central concepts of the Earth Sciences. At some level it is simply a truism: convergent plate boundaries lead to crustal thickening and drive rock uplift; a host of processes on the land surface (physical and chemical weathering, soil production, hillslope processes, fluvial and glacial erosion, etc), all dependent to some degree on climate, act in combination to erode material from the landscape; and the local (and indeed global) climate is, in turn, partly controlled by the presence and form of the underlying terrain (Figure 1). To state however, that all three are related does not address the strength of the feedbacks, the details of the underlying mechanisms, or their relative importance in different climatic and tectonic settings.

A growing body of observational evidence has pointed to the connection between tectonics and erosion in for example, the Southern Alps of New Zealand (e.g., Adams, 1980; Koons, 1989), the Alps (e.g., Bernet et al., 2003, Anders et al., 2002), Taiwan (e.g., Suppe, 1980), the Andes (e.g., Montgomery et al, 2001), the Cascades (e.g., Reiners et al., 2002, 2003) and the Olympics (Brandon et al., 1998) in Washington State, and the Himalayas (e.g., Finlayson et al., 2002) Taken together, such data suggests that at a fundamental level the basic processes of crustal deformation are inextricable from the erosional, and thus climatic, mechanisms driving exhumation (Beaumont et al., 2000).

As the understanding of each of the three components of the system has advanced, research has begun to investigate the coupling mechanisms and strengths of the interactions.

A handful of modeling studies (e.g., Koons, 1990; Beaumount et al., 1992; Masek et al., 1994; Willett, 1999) have demonstrated the effectiveness of the interactions by incorporating simple representations of orographic precipitation into coupled tectonic-surface process models. Willett (1999) for example showed the tremendous potential for the direction of the orographic rain-shadow to determine the pattern of exhumation and stress within the orogen.

Another series of papers has investigated in more detail how relief of orogens is affected by the dominant erosional process and climate feedbacks, focusing on fluvial erosion in longitudinal river profiles (e.g., Howard et al., 1994; Whipple et al., 1999; Whipple and Tucker, 1999; Tucker and Whipple, 2002; Roe et al., 2002, 2003). However these papers assumed a fixed pattern of rock uplift, and therefore omitted any tectonic response to the modeled patterns of erosion. Without understanding the nature of this tectonic response, it is unclear whether the results reflect the true sensitivity of the real system.

This paper presents a steady-state analytical solution for a simple framework which represents the three components of the system explicitly. It is similar is spirit and form to that of Whipple and Meade (2003), but because of a different formulation reaches somewhat different conclusions. Such analytical solutions provide a conceptual understanding of the coupled system's behavior, but also make important predictions which can be evaluated against observations or compared to more complete numerical models. The tectonic setting considered is that of a critical Coulomb wedge (Chappell, 1978; Davis et al., 1983; Dahlen, 1984,1990; Willett et al., 1993). The crust is assumed to behave as a plastic, frictional material. Driven by convergence and crustal accretion, surface slopes steepen until gravitational stress and basal traction are in balance while the crust is everywhere at its yield stress. The result is an orogen whose mean cross-sectional profile is wedge-shaped, maintaining a critical taper angle and changing self-similarly in response to changes in tectonic and climate forcing. We apply a model of erosion to this critical orogen that assuming that fluvial processes dominate erosion except near the divide where hillslope failure, or channel-head processes, maintain a critical hillslope angle.

It is shown in Section 2 that this model framework yields a simple and exact analytical expression for the scaling relationship for the width of the orogen as a function of climate (i.e, the precipitation rate) and tectonics (i.e., the accretionary flux), which is dependent on the parameters in the fluvial erosion law. After examining the sensitivity of the width to plausible combinations of the parameters, further analysis shows the scaling relationship is remarkably robust to relaxation of the model assumptions. We argue that this is a major reason why integrations of a numerical coupled tectonic-surface process model, presented in Stolar et al (this volume), show close agreement with the scaling relationship derived here. We end with a discussion of other aspects of the system that have been omitted and what might be the possible consequences of their omission on the behavior of the system.

2 An analytical solution

The framework we use is essentially one-dimensional (Figure 2), representing only one side a critical wedge orogen, and it is the simplest one which represents both fluvial erosion on a landscape and the tectonic response associated with critical wedge dynamics. We consider the longitudinal profile of a major trunk river, running from the foot of the orogen (at $x = L$) to a channel head (at $x = x_c$). The river channel head is assumed to be connected to the drainage divide (at $x = 0$) by a hillslope which maintains a fixed critical slope, θ_c. Since the orogen is a critical wedge, the mean topographic profile must follow a critical taper angle α_c. This is the key to the coupling of the erosion and tectonics: the total relief (i.e., fluvial plus hillslope), R, divided by the halfwidth, L, is constrained such that

$$\frac{R}{L} = \tan\alpha_c. \tag{1}$$

Tectonic forcing is in the form of a steady accretionary flux, F, which is assumed to be distributed uniformly under the wedge (i.e., underplating, e.g., Dahlen and Barr, 1989; Willett et al., 2001) so that in steady state the local rock uplift is uniform and given by

$$U = F/L. \tag{2}$$

We assume that most of the orogenic wedge is dominated by a series of transverse rivers (i.e., oriented perpendicularly to the orogen divide). Erosion rate within the river channel, E, obeys a simple fluvial erosion law:

$$E = KQ^m \left(\frac{dz}{dx}\right)^n, \tag{3}$$

where $Q(x)$ is the fluvial discharge (i.e., the fluvial discharge), and dz/dx is the along channel river profile gradient. K is the erosivity, and m and n are exponents that depend on the physical process governing the erosion (e.g., Whipple and Tucker, 1999). Other functional forms for erosion laws have been postulated which, for example, include an incision threshold (e.g., Sklar and Dietrich, 1998; Snyder et al., 2003), or regard erosion as a transport-limited process (Tucker and Whipple, 2002). Given the myriad processes acting to cause erosion in mountain rivers (e.g., Whipple et al., 2000), the stream power law is probably best regarded as quasi-empirical, justified in part by the characteristic shape of most bedrock river channels, and only in part from basic physical principles. However, the fundamental nature of the feedback studied here is unlikely to change even if erosion operates via a different process. Given the tractability of the stream power erosion law and the current developmental status of alternative representations of fluvial erosion, the incorporation of a more complex erosion law would be premature.

Such a model framework obviously makes some fairly restrictive simplifying assumptions. By construction, the modeled system has far fewer degrees of freedom by which to adjust to imposed forcing than the real one has. It is important to understand whether these other degrees of freedom are important for the response of the system. First, we consider only one side of the wedge. The framework for a two-sided wedge can be constructed by apportioning the accretionary flux so that each side maintains its own critical taper (Whipple and Meade, 2003). Doing so does not affect the sensitivity of the width to changes in forcing, provided that the recycling of eroded sediment at the orogen foot is less than complete. In seeking only steady-state solutions, the mass balance is between the accretionary flux and the integrated erosional flux: we do not worry about material accreted into the root or an isostatic response, both of which will affect the temporal evolution of the system. Next, in Sections 3 and 4 the assumptions of spatially uniform rock uplift and the fixed hillslope condition are shown to have only a small impact on the solution's sensitivity. A further factor relates to the quasi one-dimensional framework which effectively fixes the sinuosity of the major trunk rivers and further assumes that the tributaries in the drainage network and the interfluve hillslopes somehow adjust so that the major ridge profiles complement the trunk river profiles in order to maintain a critical taper. That such adjustments do in fact happen in the way we assume here is supported to some extent by the observation that many orogens are approximated by a constant mean-elevation angle. It is further supported by results of integrations of a numerical model (Stolar et al., this volume) that represents some of these extra degrees of freedom, and which yields a width and uplift response in close agreement with that presented below.

The river profile governed by Equation (3) is assumed to be anchored to the foot of the wedge, such that $z = 0$ at $x = L$. As discharge decreases towards the divide the channel slope steepens. When this slope reaches a critical value, α_c, we assume a transition from a fluvial regime governed by Equation (3) to a hillslope dominated regime, which maintains this critical slope. Letting x_c represent this transition point between erosion regimes, we can write

$$\left.\frac{dz}{dx}\right|_{fluvial} = \tan\theta_c \qquad \text{at } x = x_c \tag{4}$$

$$\frac{z_0 - z_c}{x_c - 0} = \tan\theta_c \quad \text{for } x_c < x <= 0, \tag{5}$$

where z_c denotes the elevation of the profile at x_c (see Figure 2).

Lastly, we need to specify river discharge as a function of position on the river. In building an analytical solution, we make the assumption that climatological precipitation rate, P, is uniform. This allows the discharge at a point, $Q(x)$, to be specified as directly proportional to upstream drainage area, A. We can take advantage of the empirical observation that A can be represented by an expression of the form $A = k_a x^h$ (e.g., Montgomery and Dietrich, 1992). Discharge then is given by

$$Q(x) = P k_a x^h. \tag{6}$$

Obviously precipitation is not uniform in mountainous regions, and moreover it is generally a function of mountain width and relief. It has been shown that incorporating a precipitation feedback can have a substantial impact on the modeled relief of mountain ranges (Roe et al, 2002; 2003). For now we treat it as a prescribed forcing, and we will return to this issue in Section 5 and in the Discussion. Together with an assumption of steady state, (1) to (6) form a closed set of equations which, for prescribed precipitation rate and accretionary flux (P and L), and specified erosion law parameters (K, h, m, n), can be solved to obtain the orogen width, L.

In steady-state there must be a pointwise balance between rock uplift rate and the erosion rate. So from Equations (2) and (3) we get:

$$\frac{dz}{dx} = \left(\frac{F}{2LK} \cdot \frac{1}{P^m k_a^m} \right)^{\frac{1}{n}} \cdot x^{-\frac{h}{mn}}. \tag{7}$$

The above expression can be applied at the transition point, x_c:

$$\tan\theta_{\mathrm{c}} = \left(\frac{\mathrm{F}}{2\mathrm{LK}} \cdot \frac{1}{\mathrm{P^m k_a^m}} \right)^{\frac{1}{\mathrm{n}}} \cdot \mathrm{x_c}^{-\frac{\mathrm{h}}{\mathrm{mn}}} \tag{8}$$

Next the elevation of the transition point, z_c, can be found by combining Equations (5) and (1):

$$z_c = L\tan\alpha_c - x_c\tan\theta_c. \tag{9}$$

A second expression for z_c can be derived by integrating Equation (7), subject to the lower boundary condition that $z = 0$ at $x = L$:

$$\begin{array}{ll} z_c = \left(\frac{F}{2LK} \cdot \frac{1}{P^m k_a^m} \right)^{\frac{1}{n}} \cdot \frac{1}{1-\frac{hm}{n}} \cdot \left(L^{1-\frac{hm}{n}} - x_c^{1-\frac{hm}{n}} \right) & \text{for } \frac{\mathrm{hm}}{\mathrm{n}} \neq 1 \\ z_c = \left(\frac{F}{2LK} \cdot \frac{1}{P^m k_a^m} \right)^{\frac{1}{n}} \cdot \ln(L/x_c) & \text{for } \frac{\mathrm{hm}}{\mathrm{n}} = 1 \end{array} . \tag{10}$$

For the case of $hm/n \neq 1$, and setting the right hand sides of Equations (9) and $(10)_1$ equal to each other gives:

$$\left(\frac{F}{2LK} \cdot \frac{1}{P^m k_a^m} \right)^{\frac{1}{n}} \cdot \frac{x_c^{1-\frac{hm}{n}}}{1-\frac{hm}{n}} \left\{ \left(\frac{L}{x_c} \right)^{1-\frac{hm}{n}} - 1 \right\} = L\tan\alpha_c - x_c\tan\theta_c. \tag{11}$$

Finally, on substitution from Equation (8) and rearranging:

$$\frac{1}{1-\frac{hm}{n}}\left\{\left(\frac{L}{x_c}\right)^{1-\frac{h}{mn}}-1\right\}=\frac{\tan\alpha_c}{\tan\theta_c}\left(\frac{L}{x_c}\right)-1 \tag{12}$$

For $hm/n = 1$ the equivalent expression is:

$$\ln\left(\frac{L}{x_c}\right)=\frac{\tan\alpha_c}{\tan\theta_c}\left(\frac{L}{x_c}\right)-1 \tag{13}$$

Equations (12) and (13) are implicit equations in the variable L/x_c. Therefore the solution can be found from the intersection of two curves plotting the left and right hand sides of the respective equations as a function of L/x_c. The graphical solution for the case of $hm/n \ = 1$ (Equation (12)) is shown in Figure 3. For $\alpha_c > \theta_c$ (i.e., taper angle exceeding critical slope), the two curves do not intersect. For $\theta_c > \alpha_c$ however, the curves intersect twice and there are therefore two values of L/x_c which satisfy the equations. Only one value is physical meaningful however, since by construction $x_c \leq L$. Denoting the acceptable value of L/x_cas λ, and substituting from Equation (8) gives the solution directly:

$$\left[K^{\frac{h}{n}}k_a^{\frac{hm}{n}}\tan^n\theta_c\right]L^{1+hm}\cdot F^{-1}\cdot P^m=\lambda^{hm} \tag{14}$$

which applies for both the $hm/n \neq 1$ and $hm/n = 1$ cases. Assuming α_c, θ_c, K, and the erosion law exponents remain constant as F and P vary, we can write:

$$L \propto F^{\frac{1}{1+hm}} P^{-\frac{m}{1+hm}} \tag{15}$$

This is an exact analytical scaling relationship for the model framework and approximations, and reflects the fundamental interplay between tectonics, orography, and climate (i.e., F, L, and P), mediated through critical wedge dynamics and fluvial erosion.

As is to be expected, L increases in response to an increase in accretionary flux, and L decreases for an increase in precipitation rate. Since maintaining a critical taper requires relief and width to co-vary, the scaling relationship for the total relief, R, is also given by Equation (15).

Taking log derivatives of Equation (15) shows how fractional changes in L are related to fractional changes in F and L:

$$\frac{\Delta L}{L} = \frac{1}{hm+1}\left(\frac{\Delta F}{F} - m\frac{\Delta P}{P}\right) \tag{16}$$

Therefore, for all values of the discharge exponent $m < 1$ (which most data and theoretical predictions call for), the orogen width (and total relief) are more sensitive to accretionary flux than to precipitation rate.

Interestingly, the slope exponent n does not enter into Equation (16). This is because the integral of the slope along the profile (in other words, the total relief) is strongly constrained by the imposed critical taper angle. While the lack of dependence on n is only strictly true for the formulation here (see for example Whipple and Meade, 2003), further analysis in Section 4 shows that other plausible formulations of the upper boundary condition, give rise to, at most, only a weak dependence on n. Although n does not matter for the functional sensitivity of the system, we note that it does affect the value of λ.

The sensitivity of the rock uplift rate, which in steady-state equals the exhumation rate, to tectonic and climatic forcing can also be determined. Using $U = F/L$ and Equation (15) gives:

$$U \propto F^{\frac{hm}{1+hm}} P^{\frac{m}{1+hm}} \tag{17}$$

Again n does not enter, and since $h \simeq 2$ (e.g., Montgomery and Dietrich, 1992) the exhumation rate, like the orogen width, is more sensitive to variations in accretionary flux than to variations in the precipitation rate. These conclusions differ slightly from those of Whipple and Mead (2003) because as already noted, the model formulation here is different in that the precipitation rate has been explicitly retained rather than including it in the erosivity constant, K.

It is interesting to note from Equations (15) and (17) that an increase in tectonic flux causes an increase in both exhumation rate and relief (or width). And while an increase in precipitation rate also results in an increase in exhumation rate, it leads to a decrease in relief. These contrasting effects might provide a way of differentiating the causes of relief changes, via the analysis of records of sediment production rates of thermochronometry-based estimates of erosion rates.

It is worth comparing the results of the calculations presented here to other simple models which have not included the tectonic response of the critical wedge. Several previous studies have investigated the response of relief to changes in climate and uplift by considering a longitudinal river profile of a fixed length, driven by a uniform rock uplift rate U (e.g., Whipple et al., 1999; Roe et al., 2003). By imposing a fixed length for the river profile (which is taken to represent the major trunk river in a drainage basin extending from the foot of the orogen to the divide), it is implicitly assumed that the orogen width is fixed. Thus the imposed rock uplift rate is always proportional to the implied accretionary flux, and U should be regarded as the equivalent tectonic forcing for this framework. In this "fixed-width" case, Whipple and Tucker (1999) for example, show that the fluvial relief varies as:

$$R \propto U^{\frac{1}{n}} P^{-\frac{m}{n}}. \tag{18}$$

where we have again retained the precipitation rate explicitly. And so taking log derivatives we obtain the relief sensitivity relationship:

$$\frac{\Delta R}{R} = \frac{1}{n}\left(\frac{\Delta U}{U} - m\frac{\Delta P}{P}\right) \tag{19}$$

Comparing Equation (19) to Equation (16), it is seen that the relative importance of tectonic forcing and precipitation forcing is the same as for the critical wedge. Importantly though, the absolute sensitivity is quite different and does depend on the value of n.

To constrast these different sensitivities Table 1 shows the relief response for both the critical wedge and the fixed-width cases, for three combinations of eroson law exponents representing three difference proposed mechanisms for bedrock incision (e.g., Whipple and Tucker, 1999): a) stream power ($m = 1, n = 1$, erosion proportional to rate of release of potential energy), b) unit stream power ($m = 1/2, n = 1$, stream power per unit channel width), and c) unit shear stress ($m = 1/3, n = 2/3$, erosion proportional to basal shear stress per unit channel width). For the critical wedge model and using unit shear stress, Table 1 shows that a halving of accretionary flux has the same effect as a quadrupling of the precipitation rate.

What is clear from Table 1 is that, compared to the case of a fixed width, including critical wedge dynamics provides a strong negative feedback on relief changes, thereby damping the response of the system. As also noted by Whipple and Meade (2003), this is because changes in the rock uplift rate tend to oppose changes in the width. This can be seen clearly by imagining that, from an initial equilibrium state, there is a decrease in the accretionary flux. This will tend to cause a decrease in the width of the orogen and so the accreting flux, F, will thus be distributed over a smaller width. The rock uplift rate (i.e., F/L) will therefore be larger than if L had been held fixed. The impact of this can be quite striking. Taking unit shear stress again as an example, the fixed-width model predicts that relief varies inversely with the square root of the precipitation rate. For a critical wedge however, the tectonic feedback means that the relief varies inversely with only the one-fifth power of the precipitation rate. In this case then, the relief is strongly insensitive to climate in the form of precipitation rates.

2.1 Sensitivity to model parameters

The analytical solution presented above gives the sensitivity of orogen width (and total relief) to changes in accretionary flux and precipitation rate, but makes the important assumption that everything else is held fixed as the climate and tectonic forcing changes. This is a useful idealization, but as the climate changes over a particular mountain range (perhaps to one that is stormier), it is entirely possible that the dominant process of erosion changes.

A second issue centers on whether these feedbacks are able to be evaluated in nature. It is difficult, if not impossible, to know the detailed history of the evolution of any particular mountain range. For example, it is unlikely that regional climate (in the form of precipitation rates) will ever be known to a necessary level of accuracy over a several million year time scale. One way to circumvent this would be to compare different present-day mountain ranges in different climate and tectonic settings, and to evaluate whether the differences in form between them are consistent with the feedbacks described here. This space-for-time 'swap' is possible only if other differences (e.g., lithological) do not swamp the tectonic and climate signals, or if their effects can be understood well enough to be controlled for. In this context it is useful to look at the predicted sensitivity of the mountain width to changes in the erosivity, and the critical taper and slope angles.

From field studies a wide range of erosivities have been inferred (e.g., Stock and Montgomery, 1999). Critical taper and hillslope angles also show some significant variation (e.g., Davis et al., 1983; Montgomery and Dietrich, 1992). Figure 4 shows the sensitivity of the halfwidth to changes in these model parameters, centered around a control case. In this control case, the precipitation rate is prescribed ($P_0 = 1$ myr^{-1}), as is the accretionary flux ($F_0 = 40$ m^{2}yr^{-1}). Then taking $\alpha_c = 4^o$ and $\theta_c = 40^o$, the erosivity, K_0 is selected so that for specified erosion exponents (h, m, and n), the halfwidth L_0 is 40 km. This gives a rock uplift rate of 1 mmyr^{-1}. The model parameters are then varied independently to produce the sensitivity plots in Figure 4. In reality it is likely that all three parameters are controlled at least in part by lithology, and so not strictly independent. But in the absence of quantitative understanding about how they co-vary, it is worthwhile to examine their separate effects.

Figure 4 shows the sensitivity of orogen width for the three different choices for the erosion law. The width appears least sensitive to variations in the critical slope angle (the reason for this is demonstrated in Section 4). For the critical taper angle, a doubling from 3^o to 6^o causes a reduction of about 50% in the width. Interestingly, since $R = L\tan\alpha_c$ this means that the total relief is not changing by very much as the taper angle varies. Lastly, variations in the erosivity K can have a substantial impact on the orogen width. Regression studies on observed river profiles have suggested that erosivity can vary spatially by several orders of magnitude (Stock and Montgomery, 1999). Because of the strong sensitivity of the width to the value of K, Figure 4c suggests caution in comparing widths of orogens with important lithological differences in trying to evaluate the feedbacks presented here.

3 Insensitivity of solution to rock uplift pattern

The simplifying assumptions made in Section 2 allowed for an exact analytical solution, and a demonstration of the strength of the feedback created by incorporating a tectonic response.

In the next two sections the analysis is pursued further and we show that the magnitude of the feedback is surprisingly insensitive to alternative assumptions and model frameworks.

To this point we have assumed the rock uplift is spatially uniform. This is however quite a strong constraint on the system: the precise spatial patterns of horizontal and vertical rock velocities are a function of where material is accreted and how it deforms within the orogenic wedge (e.g., Willett, 2001). Underplating and frontal-accretion (both of which can be consistent with spatially uniform rock uplift as we have assumed (Willett, 2001)) are useful concepts, but if viscous deformation and thermal coupling, or spatially varying erosion rates, are included, uniform rock uplift is not guaranteed, or expected. For example, the non-uniform temperature field within an orogen is set by topographic form and exhumation rate. This temperature field feeds back on the deformation field via the temperature-dependent viscosity (e.g., Willett, 1999).

The model framework presented here can be extended to incorporate a spatially varying rock uplift function, for which we take the following general form:

$$U = \frac{F}{L}\phi(x/L), \tag{20}$$

where ϕ is a normalized function (i.e., $\int_L^0 \phi dx = 1$). Rock uplift governed by Equation (20) scales with the accretionary flux and has been constructed such that it changes self-similarly as the wedge changes size. In Appendix A it is shown that as long as ϕ is a positive, simply integrable function, the solution can be constructed in a way that is very similar to that for uniform rock uplift, and that furthermore it gives exactly the same sensitivity of the system as Equation (15). The equivalent expression is:

$$\lambda^{hm}\phi(\lambda^{-1})^{\frac{n}{hm}} = \left[K^{\frac{h}{n}} k_a^{\frac{hm}{n}} \tan^n\theta_c\right] L^{1+hm} \cdot F^{-1} \cdot P^m \tag{21}$$

This result is an important extension of the analysis: it indicates that the details of the deformation may not be of primary importance in determining the sensitivity of a critical wedge to a change in forcing, provided that the basic pattern of rock uplift varies self-similarly. We emphasize that this result applies only to the steady-state form, and that the nature of the deformation will certainly affect how the system achieves a new steady-state in response to a change in forcing.

4 Alternative formulations of the model

We obtained the analytical solution in Section 2 by tying the major trunk rivers to the orogen divide via a critical slope. This is possible because of the essentially one-dimensional nature of the model framework. There are other possibilities. Whipple and Meade (2003) for example obtained their solution by arguing (based on data and two-dimensional land surface models with prescribed uplift) that fluvial relief is approximately proportional to total relief. While critical wedge dynamics requires that the mean topographic profile is constrained to follow the taper angle, real mountain ranges have meandering divides and complicated basin geometries. Therefore the major rivers may be only loosely tied to the average divide position. In this section the solution is generalized to show that the manner in which the major rivers are tied to the average divide position is of only secondary importance to the sensitivity of the system to changes in forcing. This result accounts for the similarity of the scaling relationship found here to that of Whipple and Meade (2003), and it also shows why the value of the slope exponent n does not contribute significantly to the sensitivity of the system.

From the schematic illustration of Figure 2, we can express the total relief generally as:

$$\text{total relief} = \text{fluvial relief} + \text{hillslope relief}. \tag{22}$$

Even if the hillslope relief depends in complex ways on other parameters in the system, it can always be written in the form $x_c\overline{\tan\theta_c}$, where x_c is still the transition point between fluvial and hillslope regimes, and $\overline{\tan\theta_c}$ denotes the average gradient of the hillslopes. We can evaluate the sensitivity of the solution to changes in x_c and $\overline{\tan\theta_c}$. Using Equation $(10)_1$ for the fluvial relief Equation (22) can be written as:

$$L\tan\alpha_c = \left(\frac{F}{LKk_a^m P^m}\right)^{\frac{1}{n}} \frac{1}{1-\frac{hm}{n}} \left(L^{1-\frac{hm}{n}} - x_c^{1-\frac{hm}{n}}\right) + x_c\overline{\tan\theta_c} \tag{23}$$

After some manipulation, this can be written as follows:

$$F \cdot L^{-(1+hm)} \cdot P^{-m} = Kk_a^m \left\{ \frac{(\tan\alpha_c - \frac{x_c}{L}\overline{\tan\theta_c})(1-\frac{hm}{n})}{1-\left(\frac{x_c}{L}\right)^{1-\frac{hm}{n}}} \right\}^n \tag{24}$$

Taking log derivatives of the above equation again gives the sensitivities for fractional changes in the various parameters. For simplicity we assume that α_c and K are constant as the forcing changes. This is not necessary, but makes the solution more easily relatable to Section 2 and Whipple and Meade (2003):

$$\frac{\Delta F}{F} - (1+hm)\frac{\Delta L}{L} - m\frac{\Delta P}{P} = n\frac{x_c\overline{\tan\theta_c}}{L\tan\alpha_c - x_c\overline{\tan\theta_c}}\left(\frac{\Delta x_c}{x_c} - \frac{\Delta L}{L} + \frac{\Delta\overline{\tan\theta_c}}{\overline{\tan\theta_c}}\right) + n\frac{\left(1-\frac{hm}{m}\right)\left(\frac{x_c}{L}\right)^{1-\frac{h}{mn}}\left(\frac{\Delta x_c}{x_c} - \frac{\Delta L}{L}\right)}{1-\left(\frac{x_c}{L}\right)^{1-\frac{h}{mn}}} \quad (25)$$

Equation (25) is complicated but useful. It can be thought of as a perturbation balance equation: in response to an imposed change in forcing (i.e., ΔP, ΔF, etc.), it shows how the combination of the other variables in the system must adjust to achieve a new equilibrium state. The left hand side of Equation (25) gives the same sensitivity as the critical slope upper boundary condition (*viz*, Equation (15)). All of the dependency on the slope exponent, n, is tied up in the right hand side of the Equation (25), which reflects changes in the upper boundary condition (i.e., the transition between fluvial and hillslope regimes).

The first term on the right hand side of Equation (25) can be considered small. The numerator in the fractional factor is the hillslope relief, and the denominator is the fluvial relief. The factor is therefore small since the latter is in general much larger than the former. This explains the relative insensitivity of the solution to changes in θ_c in Figure 4, and the factor of n explains why using simple stream power erosion (which has the highest value for n) gave the greatest sensitivity. The second term on the right hand side contains a factor x_c/L, and so might also be considered small. However it is slightly more problematic, since it is possible that $\frac{hm}{m} \simeq 1$, in which case both the numerator and the denominator can get close to zero. However l'Hôpital's rule states that in the limit of the two functions tending to zero, their ratio is equal to the ratio of their derivatives. Using this, it can be shown that in the limit of $\frac{hm}{n}$ tending to one, the second term on the right hand side tends to

$$\left[\frac{n}{ln\left(\frac{L}{x_c}\right) - 1}\right]\left(\frac{\Delta x_c}{x_c} - \frac{\Delta L}{L}\right), \tag{26}$$

and so the term is indeed always small for $x_c << L$. There are two important consequences of Equation (25). The first is that changes in the upper boundary condition have only a weak effect on the scaling relationship and the second is that, since both terms on the right hand side are small, the dependency on the slope exponent n is also weak for other formulations of the model framework.

4.1 Alternative upper boundary condition: critical discharge

The robustness of the scaling relationship to other model formulations can be illustrated concretely by choosing an alternative upper boundary condition for the hillslope processes. Instead of a critical slope, it can be assumed that a critical discharge, Q_c, is required for the formation of fluvial channels. For constant precipitation this is the same as requiring a critical upstream drainage area for channel formation. This assumption has been used (either implicitly or explicitly) in a number of studies (e.g., Whipple et al., 1999; Roe et al., 2003).

In this case then, from Equation (6), the transition point x_c is given by:

$$x_c = \left(\frac{Q_c}{P k_a} \right)^{\frac{1}{h}}. \tag{27}$$

While Equation (27) gives the transition point between the fluvial and slope-process dominated portions of the profile, one more constraint is required to tie the fluvial profile to the wedge profile at the drainage divide. To do this we assume constant slope above x_c:

$$\left. \frac{dz}{dx} \right|_{x \geq x_c} = \left. \frac{dz}{dx} \right|_{x = x_c} \tag{28}$$

where dz/dx at $x = x_c$ is given by Equation (7). There is no particular justification for Equation (28): it is not obvious what physical process would fix the slope to the value at the channel head where the critical discharge is exceeded. It is used here simply to compare the sensitivity of an alternative framework with that of the critical slope case in Section 2. We note also that Montgomery and Dietrich (1992) have suggested that channel initiation occurs where a combination of slope and discharge conditions are reached. Such a condition would also be readily incorporable into this framework.

Substituting Equation (28) into Equation (23) gives the solution for the critical discharge upper boundary condition.

$$L\tan\theta_c = \left(\frac{F}{2LK}\cdot\frac{1}{P^m k_a^m}\right)^{\frac{1}{n}} \left\{ \frac{L^{1-\frac{hm}{n}}}{1-\frac{hm}{n}} - \frac{\frac{hm}{n} x_c^{1-\frac{hm}{n}}}{1-\frac{hm}{n}} \right\} \quad \text{where } x_c = \left(\frac{Q_c}{Pk_a}\right)^{\frac{1}{h}} \tag{29}$$

Although the scaling relationship for this framework cannot be written down explicitly, the solution is readily obtained numerically. Figure 5 shows for the three different erosion laws considered earlier, there is very little difference in model sensitivity using this alternative upper boundary condition. These calculations highlight the robust nature of the scaling relationship, and suggest that despite the simplifying assumptions of the model, its implications may be quite broad and generally applicable.

5 Sensitivity to precipitation pattern

To this point the precipitation rate has been assumed to be uniform. Doing so allowed for an exact analytical solution, but in reality precipitation is highly variable in mountainous regions (e.g., Smith, 1979). The pattern of precipitation affects the pattern of river discharge, and so influences the erosion pattern via Equation (3). Imposing plausible patterns in precipitation has been shown to have an important impact on the fluvial relief in the fixed-width model reviewed in Section 2 (Roe et al., 2003). By allowing the relief to influence the precipitation (both the amount and the pattern), Roe et al. (2003) also showed that the sensitivity of the coupled system to changes in uplift rate was also affected.

We do not pursue a full-coupling with a precipitation feedback here, but we can begin to address what the impacts might be. The results of Section 2 showed that, compared to the fixed-width model, the critical wedge solution was much less sensitive to climate in the form of precipitation rates. In this section we explore the sensitivity of the two frameworks to changing the precipitation pattern. The sensitivity can be examined by combining a uniform precipitation rate with a δ-function 'spike' in the precipitation located somewhere along the river profile:

$$P(x) = p_0 + p_1\Delta \cdot \delta(x - x_0) \tag{30}$$

where x_0 is the location of the δ-function along the profile. Roe et al. (2003) show that this translates into a discharge pattern given by:

$$Q(x) = \begin{cases} p_0 k_a x^h & \text{for } 0 \leq x \leq x_{0^-} \\ p_0 k_a x^h \left[1 + \frac{h p_1 \Delta}{p_0 x_0} \left(\frac{x_o}{x}\right)^h\right] & \text{for } x_{0^-} < x \end{cases} . \tag{31}$$

It is straightforward to numerically integrate Equation (31) with the critical slope upper boundary condition (i.e., Equations (4) and (5)), and subject to the critical taper constraint. For the curves shown in Figure 6 we take $\alpha_c = 4^o$, $\theta_c = 40^o$, $p_0 = 1$ myr^{-1}, and $p_1\Delta =$ 2000 m^{2}yr^{-1} (equivalent to an increase of precipitation by 2 myr^{-1} over a 1 km portion of the channel). To facilitate comparison between curves, K is selected so that in the case of uniform precipitation (i.e., $P(x) = p_0$), L equals 40 km. This gives a total relief of ~2800 m. The total relief can then be calculated as a function of the location of the precipitation spike, x_0 for the three different erosion laws. For comparison we also show the same curves for a fixed-width model. The details of this are in Roe et al., (2003), but we take $L = 40$ km,

$U = 1$ mmyr^{-1}, $x_c = 400$ m, and in the same way select K so the fluvial relief equals 2800 m for $P = p_0$.

The response of the critical wedge model is similar to that of the fixed-width model in that the sensitivity of the relief to precipitation increases with the proximity of the anomaly is to the divide. As noted in Roe et al. (2003), in the fixed-width case, fractional changes in discharge cause fractional changes in slope of the opposite sign, and so the absolute changes in the slope are largest where the slopes are largest. Figure 6 shows that this also applies to the critical wedge model. An exception is seen for the stream power case for $x_0 <\sim 1500$ m. When x_0 becomes less than the transition point x_c the only effect is that, as seen in Equation (31), the amplitude of the discharge decreases as x_0 moves towards the divide. This effect is an artifact of having used a δ-function to test the sensitivity, and is likely unimportant in reality.

The overall impression from Figure 6 is that, like the case for the uniform precipitation, the critical wedge model is less sensitive to the pattern of precipitation than the fixed-width model. Nonethless, the precipitation anomaly chosen here is quite moderate compared to observations, so Figure 6 suggests that the feedback between the precipitation pattern and relief may well be important.

These results should be interpreted cautiously. Importantly, the model assumes that the rock uplift is uniform. Willett (1999) for example showed that imposing a rain shadow in a orogen model incorporating lithospheric deformation causes exhumation to become focussed on the wet-side of the orogen. The results in this paper show that the sensitivity of the relief changes significantly in going from a fixed-width model to a critical taper model, and it is equally possible that if the physics of the lithospheric deformation can accommodate a localized response to a precipitation pattern, the sensitivity of the total relief may be quite different again.

6 Discussion and Conclusions

Critical wedge dynamics provide a powerful negative feedback on the response of an orogen to tectonic and climate forcing. The self-similar growth implicit in critical wedge theory couples orogen height to width and, for constant mass flux, directly links rock uplift rate and orogen width. Changes in tectonic or climatic forcing therefore, produce a subdued response in the relief since the system requires concomitant changes in orogen width and rock uplift rate. This paper derived an analytical solution for the response of the orogen width to changes in tectonic forcing (as represented by an accretionary flux) and climate (as represented by the precipitation rate). The strength of the feedback depends on the parameters in the fluvial erosion law. For choices most commonly suggested by theory and observations, the orogen width and exhumation rate are both more sensitive to tectonic forcing than to climate. And in contrast to the case where the width of the orogen is prescribed, the sensitivity of the solution does not depend on the value of the slope parameter n in the erosion law.

While an analytical solution can only be obtained for a critical-gradient hillslope condition, we also showed that the scaling relationship is at most weakly dependent on both the value of n and the way that the major trunk-river profiles connect to the drainage divide. It was also shown that the pattern of rock uplift does not matter for the sensitivity provided that it is integrable, and that it changes self-similarly as the orogen size changes. The analyses are important in that they suggest that the results may be quite generally applicable and not just a consequence of the model assumptions. These results are further supported by integrations of a coupled tectonics-surface process model (Stolar et al (this volume)), which although it is a much more complex system with many ways to adjust to changes in forcing, has a sensitivity in close agreement with that predicted by the analytical results.

It is important to emphasize the limitations and caveats of the solution. It implicitly assumes, for example, that as the forcing changes the physics governing erosion remains unchanged. The relative importance of different erosional processes may well change with climate, particularly with changes in storminess (e.g., Costa and OConner, 1995; Tucker and Bras, 2000; Snyder, 2003).

Another complication would be the presence of active glaciers, although the same feedback ought to exist. Existing models of glaciation at the landscape scale asssume erosion which scales with the rate of glacier sliding (e.g., MacGregor et al., 2000; Tomkin and Braun, 2002), both of which tend to increase with precipitation rate. However in an orogen with significant glaciated areas, it is quite possible that because of the very different effectiveness of glacial and fluvial erosion (e.g., Hallet, 1996), the integrated erosion rate over the orogen may be more sensitive to summertime temperature (to the degree that it dictates the permanent snow line) than to precipitation.

A further possibility not addressed in the calculations presented here is that the response of the system depends on the strength of the rain shadow (e.g., Willettt, 1999; Whipple and Meade, 2003). As an orogen grows it is to be expected that, all else being equal, the strength of the rain shadow increases, both because the average ascent and descent on the windward and leeward flanks of the orogen respectively, would be expected to increase, but also because more storms would be blocked on the windward side (e.g., Smith, 1979). An additional factor is that the results in Section 5 and in Roe et al., (2003) showed that the pattern of precipitation, and in particular the near-divide precipitation is important.

A long term objective of this work is to be able to reconcile observed topographic forms with the climatic and tectonic settings which have given rise to them. Ongoing studies into each of these three components of the Earth system continually yields new insights, a result of which is that new physical mechanisms and uncertainties emerge. A major challenge for the field therefore, is to understand whether there are aspects of this enormously complex system which behave in robust and predictable ways, or do the myriad feedback pathways and nonlinear interactions preclude a quantitative understanding of the system? All of the caveats noted above are reasons why any particular orogen might not behave according to Equation (15), or why different orogens might behave differently from each other. On the other hand, the fundamental nature of the feedback does not depend on the system being governed by the strict definitions of critical wedge dynamics. Provided the steady-state orogen width has a tendency to increase in response to an increase in accretionary flux (or a decrease in precipitation rate), the feedback will tend to operate to damp the system response to changes in forcing. Moreover taking one particular framework, we have shown that the feedback is strong, that it's magnitude is insensitive to some of the details of the model formulation and furthermore, that it captures the behavior of a more complex numerical model with many more degrees of freedom by which to adjust (Stolar et al. (this volume)). The results lend confidence that aspects of the system are indeed robust and comprehensible, and that it therefore remains a worthwhile, if challenging, research goal to pursue an understanding of how climate, erosion, and tectonics have combined to sculpt Earth's landscapes.

Acknowledgements

The authors are grateful to Kelin Whipple, David Montgomery and Bernard Hallet for stimulating and helpful conversations.

Appendix A: Solution for non-uniform uplift rate

For the framework of Section 2 the total relief in the wedge, R, can be written as

$$R = L\tan\alpha_c = \int_L^{x_c} \frac{dz}{dx} dx + x_c \tan\theta_c. \tag{32}$$

Taking the rock uplift rate given by Equation (20), and requiring a pointwise balance between erosion and this uplift function and rearranging for dz/dx, gives an equation similar to Equation (7):

$$\frac{dz}{dx} = \left(\frac{F}{2LK} \cdot \frac{1}{P^m k_a^m}\right)^{\frac{1}{n}} \cdot [\phi(x/L)]^{\frac{1}{n}} \cdot x^{-\frac{h}{mn}}, \tag{33}$$

which upon substitution into Equation (32) gives:

$$L\tan\alpha_c = x_c\tan\theta_c + \int_L^{x_c} \left(\frac{F}{LKP^m k_a^m}\right)^{\frac{1}{n}} [\phi(x/L)]^{\frac{1}{n}} x^{-\frac{hm}{n}} dx. \tag{34}$$

Next we make a substitution of variables $y = L/x$:

$$L\tan\alpha_c = x_c\tan\theta_c + \left(\frac{F}{LKP^m k_a^m}\right)^{\frac{1}{n}} [\phi(x/L)]^{\frac{1}{n}} \int_1^{\frac{x_c}{L}} L^{-\frac{hm}{m}} \phi(y)^{\frac{1}{n}} y^{-\frac{hm}{n}} dy. \tag{35}$$

Finally, using Equation (33) with $x = x_c$, and rearranging gives:

$$\left(\frac{L}{x_c}\right) \frac{\tan\alpha_c}{\tan\theta_c} - 1 = [\phi(x_c/L)]^{-\frac{1}{n}} \left(\frac{x_c}{L}\right)^{\frac{hm}{n}-1} \int_1^{\frac{x_c}{L}} \phi(y)^{\frac{1}{n}} y^{-\frac{hm}{n}} dy \tag{36}$$

Provided $\phi(y)$ is an integrable function, then like the uniform rock uplift solution, Equation (36) is an implicit equation in L/x_c. The solution can be written as $L/x_c = \lambda$, with the value of λ to be found. Using Equation (33) with $x = x_c$, and rearranging gives:

$$\lambda^{hm} \phi(\lambda^{-1})^{\frac{n}{hm}} = \left[k_a^{\frac{hm}{n}} \tan^n\theta_c K^{\frac{h}{n}}\right] L^{1+hm} \cdot F^{-1} \cdot P^m. \tag{37}$$

References

Abramowitz, M., and I. A. Stegun, 1965: Handbook of mathematical functions with formulas, graphs, and mathematical tables. Dover publications, New York, pp 1046.

Adams, J., 1980: Contemporary uplift and erosion of the Southern Alps, New Zealand. *Geol. Soc. Amer. Bull.* Part I, **91**, 1-114.

Anders, A.M., D.R. Montgomery, and B. Hallet, 2002: Comparing spatial variations in precipitation and erosion index to differences in long term exhumation along the European Alps, GSA Abstracts with Programs, Annual Meeting, **34**, 6, pg 108.

Beaumont, C., H. Kooi, and S.D. Willett, 2000: Couple tectonic-surface process models with applications to rifted margins and collisional orogens. In Summerfield, M., ed, *Geomoprh. and Glob. Tect.*, Wiley, Chichester, U.K., 29-56.

Bernet, M., M.T. Brandon, J.I. Gaver, B.R. Molitor, B.R., 2003: Fundamentals of detrital zircon fission-track analysis for provenance and exhumation studies with examples from the European Alps. In review for Geological Society of America Special Paper, "Detrital Thermochronlogy - Exhumation and Landscape Evolution of Mountain Belts", Matthias Bernet and Cornelia Spiegel (editors)

Chapple, W.M., 1978: Mechanics of thin-skinned fold and thrust belts *Geol. Soc. Am. Bull*, **89**, 1189-1198.

Costa, J. E. and J. E. O'Conner, 1995: Geomorphically effective floods. In Costa, J. E., A. J. Miller, K. W. Potter, and P. R. Wilcock (eds), *Natural and Anthropogenic influences in fluvial geomorphology*, Geophys. Monogr. Ser. vol 89, p45-56. Am. Geophys. U., Washington, DC.

Dahlen, F.A., 1984: Noncohesive critical Coulomb wedges: An exact solution, *J. Geophys. Res.*, **89**, 10125-10133.

Dahlen, F.A, 1990: Critical taper model of fold-and-thrust belts and accretionary wedges. *Annu Rev. Earth Planet. Sci.*, **18**, 55-99.

Davis, D., J. Suppe, and F.A. Dahlen, 1983: Mechanics of fold-and-thrust belts and accretionary wedges. *J. Geophys. Res.*, **88**, 1153-1172.

Finlayson, D.P., D.R. Montgomery, and B. Hallet, 2002: Spatial coincidence of rapid inferred erosion with young metamorphic massifs in the Himalayas. *Geology*, **30**, 219-222.

Howard, A.D., W.E. Dietrich, and M.A. Seidl, 1994: Modeling fluvial erosion on regional to continental scales: Journal of Geophysical Research, **99**, 13971-13986.

MacGregor, K. R., R. S. Anderson, S. P. Anderson, and E. D. Waddington, 2000: Numerical Simulations of glacial-valley longitudinal profile evolution. *Geology*, **28**, 1031-1034.

Montgomery, D.R., and W.E. Dietrich, 1992, Channel initiation and the problem of landscape scale: Science, **255**, 826-830.

Reiners, P.W., T.A. Elhers, J.I. Garver, S.G. Mitchell, D.R. Montgomery, J.A. Vance, and S. Nicolescu, 2002: Late Miocene exhumation and uplift of the Washington Cascade Range. *Geology*, **30**, 767-770.

Reiners, P.W., T.A. Ehlers, S.G. Mitchell, and D.R. Montgomery, 2003: Coupled spatial variations in precipitation and long-term erosion rates across the Washington Cascades. *Nature*, **426**, 645-657.

Roe, G. H., D. R. Montgomery, and B. Hallet, 2002: Effects of Orographic Precipitation Variations on the Concavity of Steady-State River Profiles. *Geology*, **30**, 143-146.

Roe, G. H., D. R. Montgomery, and B. Hallet, 2003: Orographic precipitation and the relief of mountain ranges. *J. Geophys. Res*, doi:10.1029/2001JB001521.

Sklar, L., and W.E. Dietrich, 1998: River longitudinal profiles and bedrock incision models: Stream power and the influence of sediment supply. In Tinkler, T. J., and E. E. Wohl (eds), *Rivers over Rock: Fluvial processes in bedrock channels.* Geophys. Monogr. Ser. 107, p237-260., Am. Geophys. U., Washington DC.

Smith, R. B., 1979: The influence of mountains on the atmosphere. In Saltzman, B. (ed.), *Advances in Geophysics*, 21, p87-230. Academic Press, New York.

Snyder, N. P., K. X. Whipple, G. E. Tucker, and D. J. Merritts, 2000: Landscape response to tectonic forcing: Digital elevation model analysis of stream profiles in the Mendocino triple junction region, northern California. *Geological Society of America Bulletin*, **112**, 1250-1263.

Snyder, N.P., K.X. Whipple, G.E. Tucker, and D.M. Merritts, 2003: Importance of a stochastic distribution of floods and erosion thresholds in the bedrock river incision problem, *Journal of Geophysical Research*, **108 (B2)**, 2117, doi:10.1029/2001JB001655.

Stock, J.D. and D.R. Montgomery, 1999: Geologic constraints on bedrock river incision using the stream power law, *J. Geophys. Res.*, **104**, 4983-4993.

Stolar, D, S.D. Willett, and G.H. Roe, 2004: Integrations of a coupled tectonics-surface process model. Submitted to A.G.U. special Penrose volume.

Suppe, J., 1980: A retrodeformable cross section of northern Taiwan. *Geol. Soc. China Proc.*, **23**, 46-55.

Tomkin, J. H., and J. Braun, 2002: The influence of alpine glaciation on the relief of tectonically active mountain belts. *Am. J. Sci.*; **302**, 169-190.

Tucker, G. E., and R. L. Bras, 2000: A stochastic approach to modeling the role of rainfall variability in drainage basin evolution. *Water Res. Res.*, **36**, 1953-1964.

Tucker, G. E., and K. X. Whipple, 2002: Topographic outcomes predicted by the stream erosion models: sensitivity analysis and intermodel comparison. *J. Geophys. Res*, **107**, doi: 10.129/2001JB000162.

Whipple, K.X., E. Kirby, and S. H. Brocklehurst, 1999: Geomorphic limits to climate-induced increases in topographic relief. *Nature*, **401**, 39-43.

Whipple, K.X. and G. E. Tucker, 1999: Dynamics of the stream-power river incision model: implications for height limits of mountain ranges, landscape response time scales, and research needs: *J. Geophys. Res.*, **104**, 17,661-17,674.

Whipple, K.X., G.S. Hancock, and R.S. Anderson, 2000. River incision into bedrock: Mechanics and the relative efficacy of plucking, abrasion, and cavitation. *GSA Bulletin.* **112**, 490-503.

Whipple, K.X. and B.J. Meade, 2004: Dynamic coupling between erosion, rock uplift, and strain partitioning in two-sided, frictional orogenic wedges at steady-state: an approximate analytical solution. *In press J. Geophys. Res.*

Willett, S.D, C. Beaumont, and P. Fullsack, 1993: Mechanical model for the tectonics of doubly-vergent compressional orogens. *Geology*, **21**, 371-374.

Willett, S. D., 1999: Orogeny and orography: The effects of erosion on the structure of mountain belts. *J. Geophys. Res.*, **104**, 28957-28981.

Tables

Mechanism	m	n	h	Critical wedge		Fixed-width	
				Tectonics	Precipitation	Tectonics	Precipitation
				$F^{\frac{1}{1+hm}}$	$P^{-\frac{m}{1+hm}}$	$U^{\frac{1}{n}}$	$P^{-\frac{m}{n}}$
Stream Power	1	1	2	$\frac{1}{3}$ (23)	$-\frac{1}{3}$ (23)	1 (100)	-1 (100)
Unit Stream Power	$\frac{1}{2}$	1	2	$\frac{1}{2}$ (41)	$-\frac{1}{4}$ (19)	1 (100)	$-\frac{1}{2}$ (41)
Unit Shear Stress	$\frac{1}{3}$	$\frac{2}{3}$	2	$\frac{3}{5}$ (60)	$-\frac{1}{5}$ (15)	$\frac{3}{2}$ (183)	$-\frac{1}{2}$ (41)

Table 1: Sensitivity of relief of an orogen for critical wedge model, and fixed-width model, described in the text, for three different proposed erosion mechanisms. m and n are discharge and slope exponents, respectively, in the erosion law, and h is the Hack's law exponent. The ratios in the last four columns are the values of the exponents for the tectonics and precipitation sensitivities, for the appropriate combinations of h, m, and n. To illustrate these sensitivities, the figures in parentheses are the percentage increases in relief due to either a doubling of the tectonic forcing, or a halving of the precipitation rate.

Figures

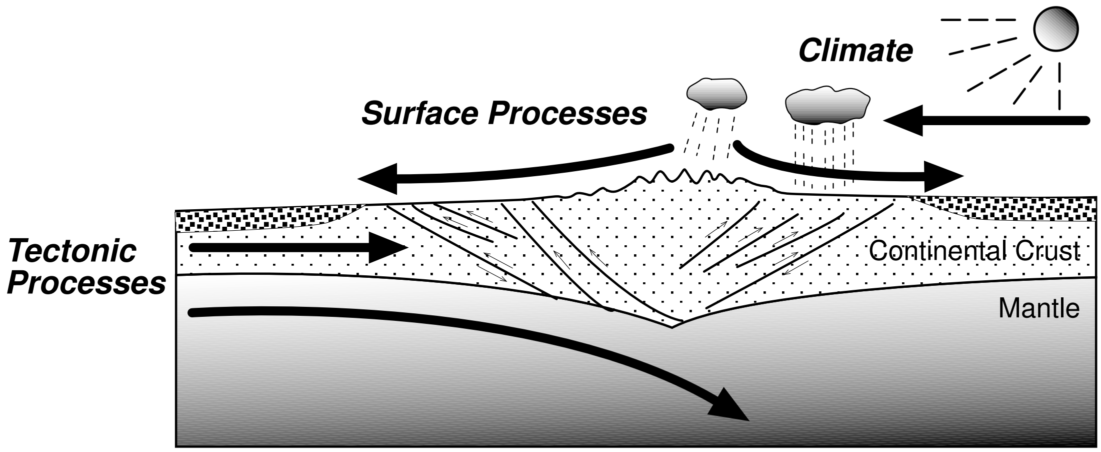

Figure 1: Schematic illustration of the process involved in interplay between climate, tectonics, and erosion (after Willett, 1999).

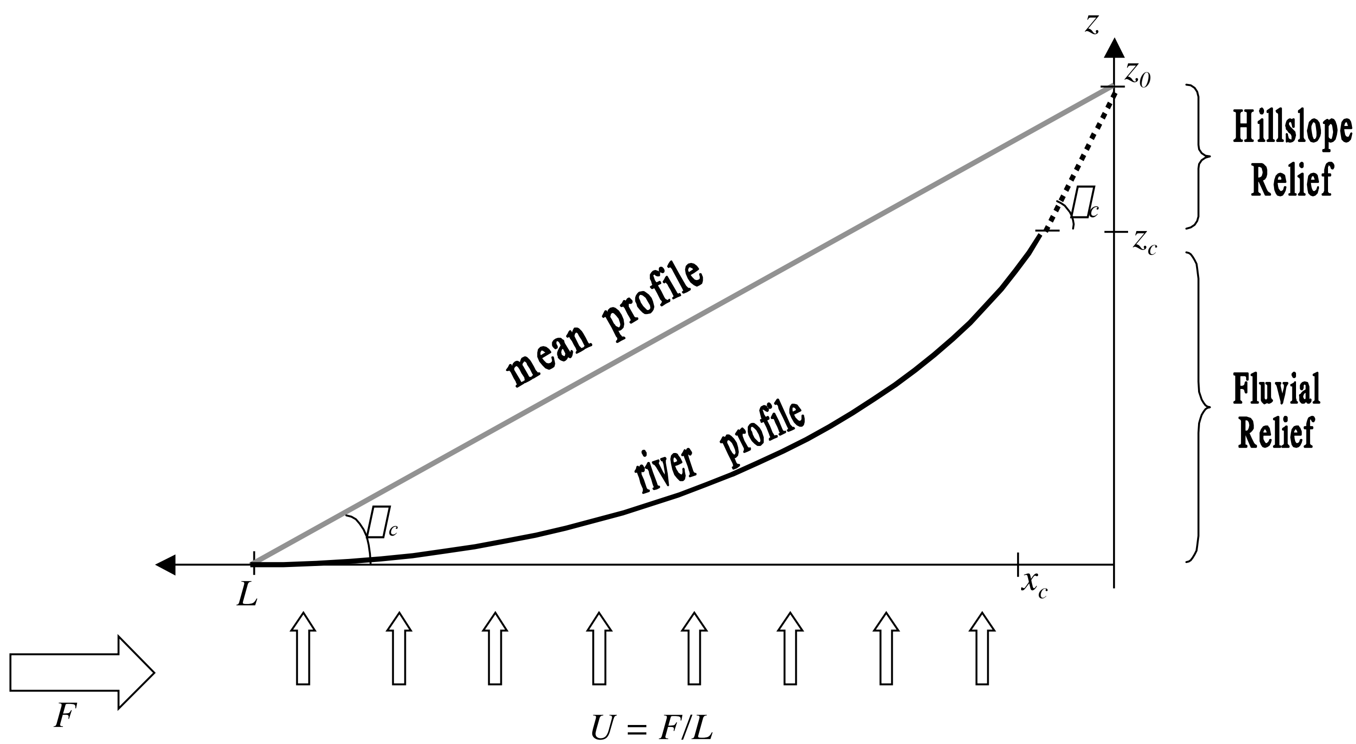

Figure 2: The model framework. The accretionary flux is distributed uniformly as rock uplift over the domain. Togther the fluvial and hillslope relief equal the total relief which is constrained to maintain a critical taper angle

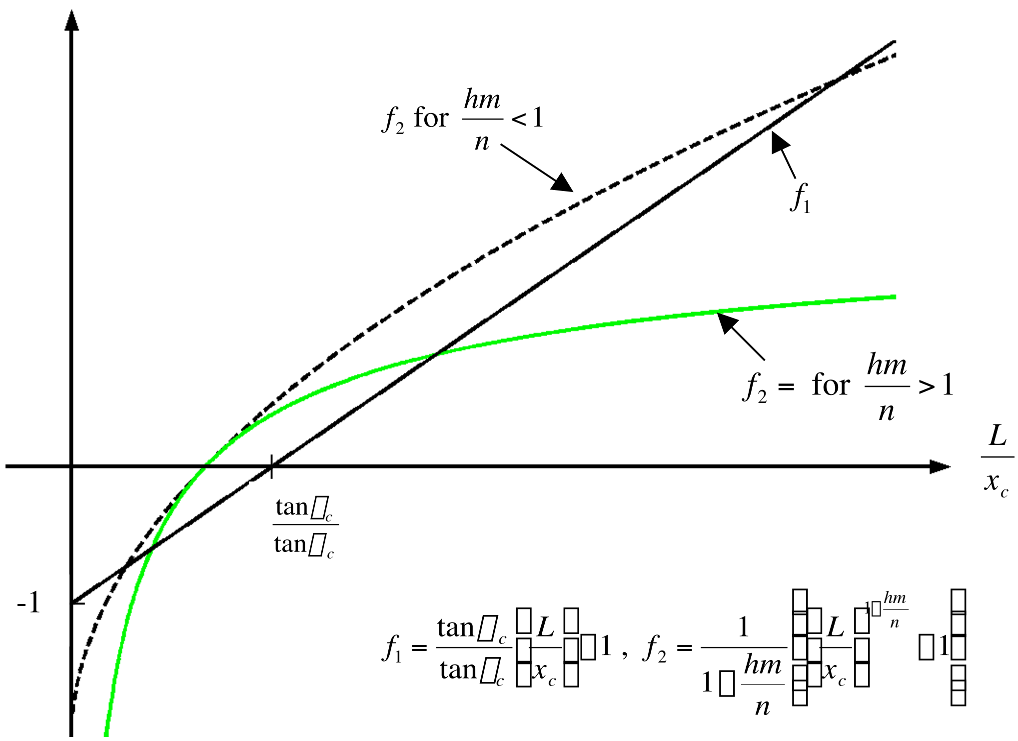

Figure 3: Graphical solution to Equation (12). f_1 and f_2 are the left and right hand sides of Equation (12) respectively, plotted as a function of L/x_c. The solution to Equation (12) is given by the intercept of the two functions. Note that two curves for f_2 are plotted, due to the different behaviour of the function depending on the sign of $(hm/n - 1)$.

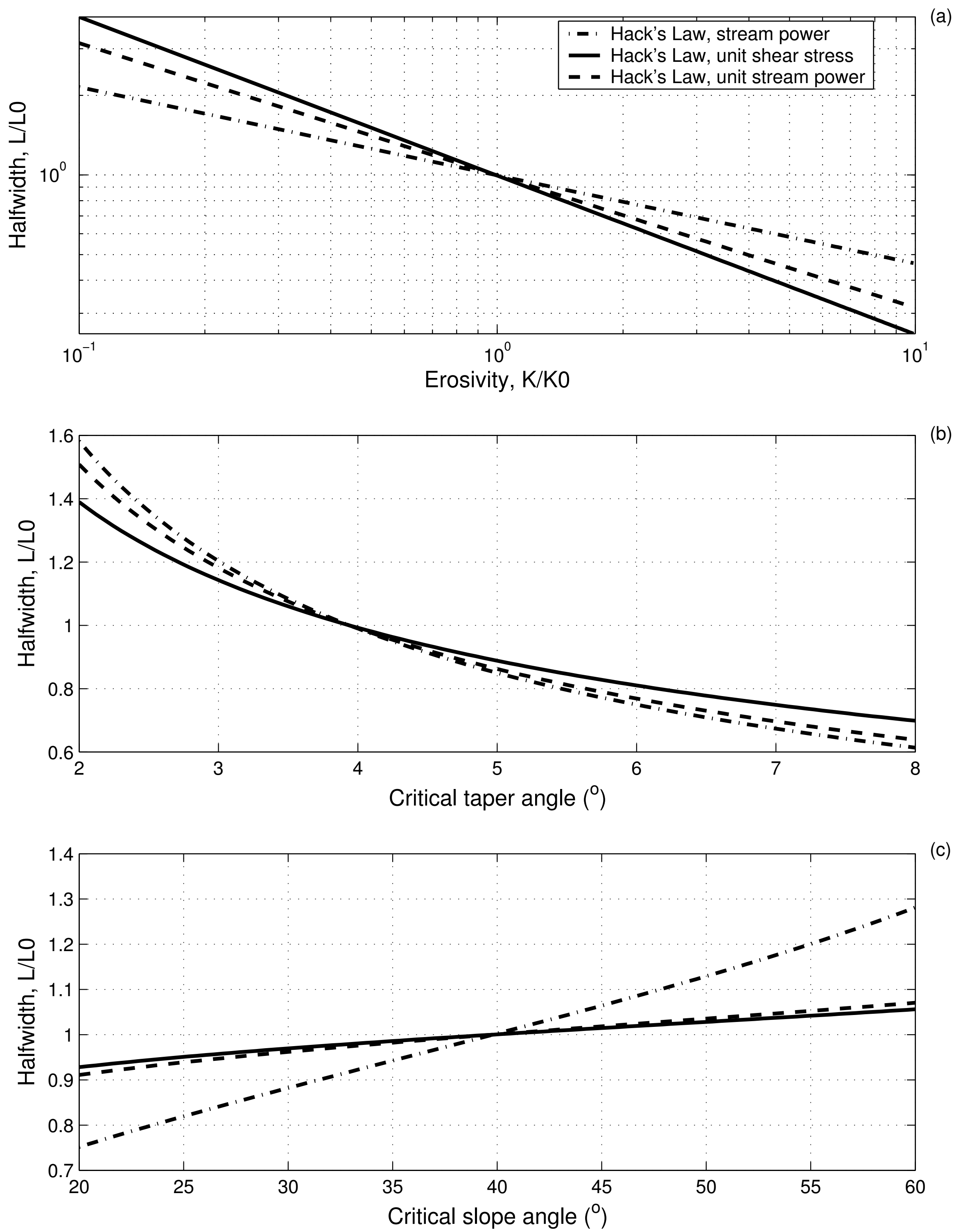

Figure 4: Sensitivity of the orogen width to model parameters, a) erosivity K, b) critical taper angle, α_c, and c) critical slope angle θ_c. The details of the parameters used in these results are given in the text.

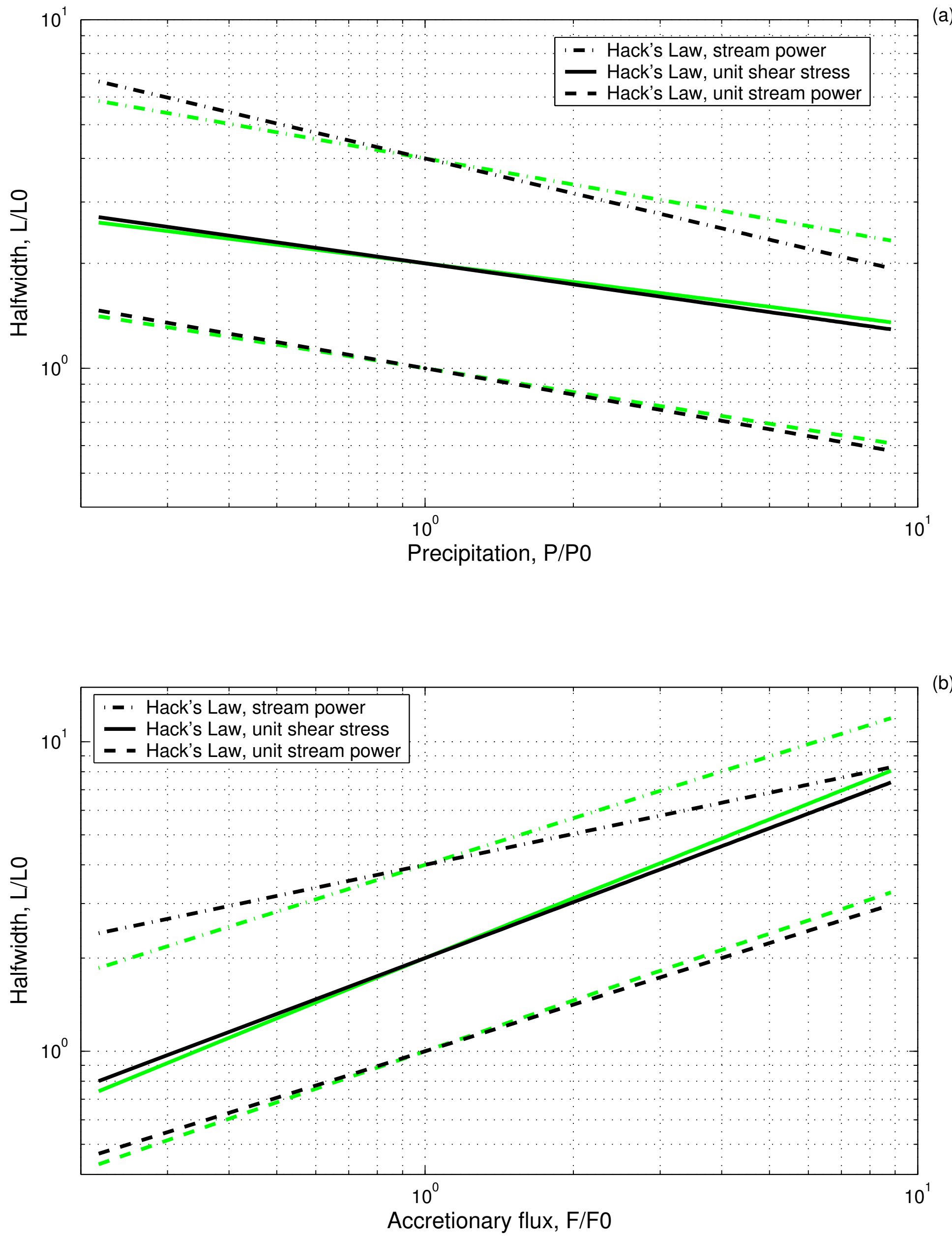

Figure 5: Sensitivity of the solution to boundary conditions. a) width as a function of precipitation, b) width as a function of accretionary flux. The black lines are for a critical-slope upper boundary condition, and the gray lines are for a critical-discharge upper boundary condition. The line style indicated in the legend denotes the three different erosion laws tested. For clarity on the plot, the dashed lines have been shifted on the y-axis by a factor of two. The figure highlights the insensitivity of the feedback to different model formulations.

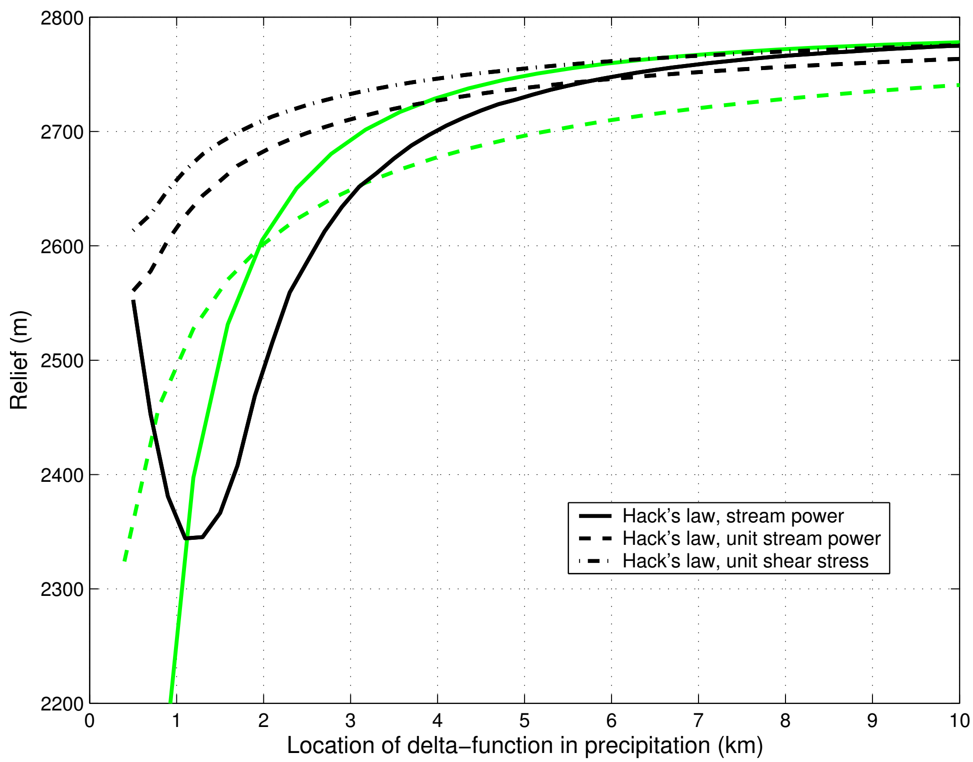

Figure 6: Sensitivity of relief to imposed δ-function in precipitation. The graphs plots relief as a function of the location of the δ-function. $x = 0$ is the drainage divide. Lines plotted show the total relief from the critical wedge model for the three different choices of erosion law (black lines), and for comparison the fluvial relief for the fixed-width model (gray lines). Note for the fixed-width model, unit stream power and unit shear stress have the same sensitivity. For the critical wedge model and the stream power erosion law, the minium in relief occurs when the transition point x_c becomes greater than the location of the δ function, x_0. For model details see text.